OATAO
Open Archive Toulouse Archive Ouverte

Open Archive Toulouse Archive Ouverte (OATAO)

OATAO is an open access repository that collects the work of Toulouse researchers and makes it freely available over the web where possible.

Any correspondence concerning this service should be sent to the repository administrator: staff-oatao@inp-toulouse.fr

Chemical Evolution in the Substrate due to oxidation: A Numerical Model with Explicit Treatment of Vacancy Fluxes

N. Bertrand[1now at 2,b], C. Desgranges[1,a], M. Nastar[1,c], G. Girardin[2,d], D. Poquillon[3,e], D. Monceau[3,f]

[1]CEA-Saclay, 91 191 Gif-sur -Yvette Cedex, France

[2]AREVA-NP, Technical Center, 71205 Le Creusot Cedex, France

[3]CIRIMAT CNRS/UPS/INPT, ENSIACET, 31077 Toulouse Cedex 4, France

[a]clara.desgranges@cea.fr, [b]nathalie.bertrand@areva.com, [c]maylise.nastar@cea.fr, [d]gouenou.girardin@areva.com, [e]dominique.poquillon@ensiacet.fr, [f]daniel.monceau@ensiacet.fr

Abstract. To get a better understanding of oxidation behavior of Ni-base alloys in PWR primary water, a numerical model for oxide scale growth has been developed. The final aim of the model is to estimate the effects of possible changes of experimental conditions. Hence, our model has not been restricted by the classical hypothesis of quasi-steady state and can consider transient stages. The model calculates the chemical species concentration profiles, but also the vacancy concentration profiles evolution in the oxide and in the metal as a function of time. It treats the elimination of the possible supersaturated vacancies formed at the metal/oxide interface by introducing a dislocation density at the interface and in the metal bulk. This latter density can be related to the cold-working state. Its effect on the vacancy profile evolution is studied in the case of a pure metal. Eventually an extension of the present model to the oxidation of Ni-base alloys is discussed regarding a recent vacancy diffusion model adjusted on Ni-base alloys.

Introduction

The understanding of the oxidation behavior of Ni-base alloys in PWR primary water is of major importance due to the cations released due to corrosion of the steam generators which is a source of the radioactivity of the primary circuit. Moreover, the oxidation process is the reason of the initiation of intergranular stress corrosion cracking (IGSCC) in alloys 600, 82 and 182.

The oxide layers formed on alloy 600, and alloy 690, in primary PWR water at 360°C are similar [1] in nature but two or three times thicker for the alloy 600. A typical oxide scale is composed of a thin Cr-rich inner layer at the metal/oxide interface, probably made of Cr_2O_3, under a Cr-rich oxide layer composed of a mixed Fe-Ni-Cr oxide of spinel structure such as $NiCr_2O_4$ [2]. Moreover, an outer Cr free oxide layer consists of crystallites spread over the surface containing Fe and Ni only. Extensive studies [2-10] on the oxidation processes of Ni-base alloys in PWR primary coolant have demonstrated the importance of characterizing and modeling the initial stages of oxidation. Indeed, oxidation experiments on Ni-base alloys have demonstrated the occurrence of two different types of base metal damage: penetration of oxygen in the grain boundaries and the formation of a Cr-depleted metal layer immediately below the Cr_2O_3 oxide inner sub-layer as a consequence of the selective oxidation of Cr [1]. Nevertheless, the simple calculation of the mean free path of the Cr diffusion coefficient in the alloy from experimental profile [3] leads to a value a few orders of

magnitude greater than the theoretically calculated one [11, 12]. Similar Cr-depletion has been observed by Seo and Sato [13, 14] in gaseous atmospheres at higher temperature (450-550°C). There is a continuing debate about the nature of the mechanisms involved in this accelerated diffusion. Several hypotheses have been proposed to explain this accelerated diffusion, such as the presence of a perturbed layer near the alloy surface that contains small grains and large density of defects [3] or a massive injection of vacancies into the metal caused by the growth of the oxide layer [13-15].

Therefore, modeling the oxide scale growth with an explicit treatment of the vacancy fluxes in the oxide and in the substrate should lead to a better understanding of the evolutions in the substrate and of the possible origin of the IGSCC in alloy 600. And then, it will allow to evaluate the safety margin of the alloy 690.

For a cationic transport mechanism, every models derived from Wagner's theory assume that all the vacancies are annihilated at the interface. Hence, the interface motion relative to the metal lattice is straightforwardly deduced from the quantity of metal recession due to oxide growth, and as a result, the movement of the interface follows parabolic kinetics. On the other hand, as revealed by voids formation which are sometimes evidenced, vacancies are not always all annihilated at the interface [16]. Indeed it should be more appropriate to consider that vacancies are neither all eliminated at interface nor all injected in the metal, but rather partially annihilated at the interface and hence partially injected. Pieraggi *et al.* [17] have linked the capacity of interfaces to annihilate incoming vacancies to the ability for interface dislocations to climb. In the case of pure cationic growing scales, they showed that cationic vacancies could only be annihilated by climbs of disorientation or misfit dislocations in the metal, these latter being energetically favored.

The aim of this work is then to build a numerical model to simulate an oxide scale growth taking into account vacancies as non-conservative species. This model should be able to calculate the evolutions of concentration profiles of the species and of their point defects in the oxide and in the substrate. Hence, this model called EKINOX (Estimation KINetics OXidation) should be an innovative tool for a better understanding of the oxidation behavior of Ni-base alloys in PWR primary water.

Presentation of the numerical model EKINOX for a pure metal M forming an oxide MOγ

General description. The numerical model EKINOX is a one dimensional model that simulates the growth of an oxide layer whose composition is MO_γ, using the explicit finite differences method as the integration algorithm. A description of the model EKINOX has already been given in [18]. It is divided into Ns layers of equal initial thickness. The substrate of metal M extends from the first to the Ni^{th} layer and the oxide scale extends from the layer $Ni+1$ to the layer Ns $_\gamma$. In the oxide, the two sub-lattices are considered for the cations and for the anions, whereas only one lattice is considered in the metal. Each sublattice is occupied either by the corresponding chemical species (metal M, oxygen O) or by the corresponding vacancies (V_M , V_O). In the present version of the model, oxygen is supposed to be insoluble in the substrate. The model EKINOX does not make the classical steady-state hypothesis, and is thus able to study transient stages, evolutions in a finite size substrate due to oxidation and effects of microstructural changes, such as grain growth or dislocation density evolution.

Equations governing the evolution of the concentration profiles. Species transport is calculated from slab to slab with the explicit treatment of vacancy fluxes, following Fick's first law:

$$J_{V_k}^n = -\frac{D_{V_k}^n}{\Omega^n} \frac{X_{V_k}^{n+1} - X_{V_k}^n}{\dfrac{e^n + e^{n+1}}{2}} \tag{1}$$

Equation 1 gives the flux $J_{V_k}^n$ of vacancies V_k from slab n to $n+1$ in the reference frame corresponding to the nature of the considered slab n. e^n is the thickness of the layer n, $X_{V_k}^n$ is the concentration in sites fraction of the vacancies V_k in the layer n, $D_{V_k}^n$ is the diffusion coefficient of the vacancies V_k in the layer n and Ω^n is the molar volume of the layer n. Then, the variation of concentration $X_{V_k}^n$ of vacancies V_k in the layer n is given by the Eq. 2. A mirror condition is considered in the slab 1 which means that the model calculates the oxidation of a finite size sample.

$$\dot{X}_{V_k}^n = \frac{dX_{V_k}^n}{dt} = -\Omega^n \frac{J_{V_k}^n - J_{V_k}^{n-1}}{e^n} \tag{2}$$

Interface motion. For the layers beside the interfaces (*Ni, Ni+1* and *Ns*) the conservation equation (Eq. 2) leads to a thickness variation of the slabs. Thus both interfaces are mobile, because of cationic and anionic fluxes. The corresponding variation with time of the slab thickness, e^{Ns} and $\dot{e}^{Ni+1}$, is given by the Eq. 3 and 4, where $X_M^{eq^s}$ and $X_{V_M}^{eq^s}$ refer to the equilibrium concentration of ,respectively , cations and cationic vacancies at the surface of the oxide, $X_O^{eq^i}$ and $X_{V_O}^{eq^i}$ refer to the equilibrium concentration of, respectively, anions and anionic vacancies at the metal/oxide interface. The anionic oxide growth leads to a recession of the metal layer thickness e^{Ni} in the ratio of the molar volumes, that is to say the Pilling-Bedworth Ratio ($\Omega_{MO_\gamma}/\Omega_M$) :

$$\dot{e}^{Ns} = \Omega^{Ns} \frac{J_M^{Ns-1}}{X_M^{eq^s}} = -\Omega^{Ns} \frac{J_{V_M}^{Ns-1}}{1 - X_{V_M}^{eq^s}} \tag{3}$$

$$\dot{e}^{Ni+1} = \frac{\Omega^{Ni+1}}{\gamma} \frac{-J_O^{Ni+1}}{-X_O^{eq^i}} = \frac{\Omega^{Ni+1}}{\gamma} \frac{J_{VO}^{Ni+1}}{1 - X_{V_O}^{eq^i}} \tag{4}$$

The implementation of the algorithm for moving boundaries is described in [19].

Different hypothesis at the interfaces. At the surface of the oxide scale, the thermodynamic equilibrium is supposed to be reached instantaneously. At metal/oxide interface, one can either consider an instantaneous thermodynamic equilibrium or a kinetics for the transfer of metallic species from the substrate to the oxide. The flux for such a transfer is then considered to be proportional to the transfer coefficient "α" and the difference between the effective and the equilibrium concentrations for cationic vacancies at metal/oxide interface (Eq. 5) [20] :

$$J_{V_M}^{trans} = -\frac{\alpha}{\Omega^{Ni+1}} \left(X_{V_M}^{eff} - X_{V_M}^{eq^i} \right) \tag{5}$$

Vacancy treatment. Metallic vacancies are treated as non-conservative species : the total amount of vacancies evolves during the simulation. They can be eliminated in the substrate by dislocations and at the metal/oxide interface by misfit dislocations between the oxide and the substrate. The velocity of the vacancy concentration variation is given by Eq. 6 where ρ^n refers to the dislocation density in the slab n, and leads to the decrease of the corresponding layer thickness (Eq. 7) following [21].

$$\left(\dot{X}_{V_M}^n \right)_{sink} = -\frac{\rho^n}{\Omega^n} D_{V_M} \left(X_{V_M}^n - X_{V_M}^{eq} \right) X_M^n \tag{6}$$

$$\left(\stackrel{\bullet}{e^n}\right)_{sink} = -\frac{\rho^n}{\Omega^n} D_{V_M} \left(X_{V_M}^n - X_{V_M}^{eq}\right)e^n \tag{7}$$

The dislocation density is not necessarily uniform in the substrate and can decrease from the surface into t the metal bulk which corresponds better to surface cold working

Results obtained with the model EKINOX for a pure metal and discussion

To explore the consequences of various hypothesis made on the treatment of vacancies, on the shape of concentration profiles and on the oxidation kinetics, three different illustrations of calculation results obtained with EKINOX are presented in the following part. All calculations have been done with an initial number of slabs N_s =132 having a typical initial thickness of 0.25 μm.

Mixed diffusion mechanism controlling oxide scale growth. The parameters used for the calculation are given in Table 1. The cationic vacancies data are taken from the literature for the nickel oxide (NiO) growth at 1000°C [22]. The same values are arbitrarily chosen for the anionic vacancies in order to illustrate an anionic and cationic oxide scale growth with the same diffusivity for both species. The oxide scale growth kinetics is shown on Fig. 1. It is parabolic and the parabolic kinetics constant k_p is equal to 2.64 10^{-11} cm^2.s^{-1}. The interface motion is shown on Fig. 2. Both interfaces move and their displacement is symmetrical as we could expect from values given to input data.

Table.1 Input data for the simulation of an anionic and cationic diffusion controlled oxide scale growth.

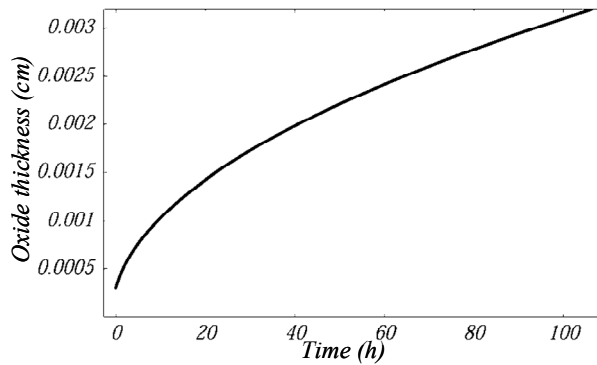| Cationic vacancies			Anionic vacancies			k_p (steady-state) (cm^2.s^{-1})
$X_{V_M}^{eq^i}$	$X_{V_M}^{eq^s}$	D_{V_M} (cm^2.s^{-1})	$X_{V_O}^{eq^i}$	$X_{V_O}^{eq^s}$	D_{V_O} (cm^2.s^{-1})	
10^{-6}	6.15 10^{-5}	1.08 10^{-7}	6.15 10^{-5}	10^{-6}	1.08 10^{-7}	2.61 10^{-11}

Fig. 1. Oxide scale growth kinetics calculated with the same diffusivity for the anions and the cations.
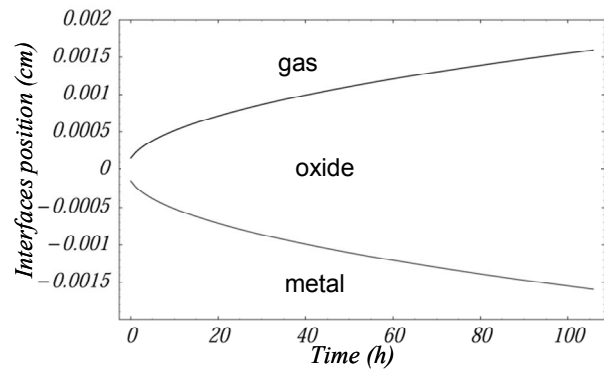

Fig. 2. Interfaces motions in the reference frame linked to the oxide lattice calculated with the same diffusivity for the anions and the cations.

Partial control of the oxide scale growth by the interfacial reaction. In this case, only cations are considered as mobile species. The cationic vacancy diffusion data are the same as in the previous case, and the transfer coefficient at the metal/oxide is chosen so that the steady-state ratio $k_p/k_l = 10^{-3}$ cm. Used parameters are summarized in Table 2. For this calculation, the initial concentration profile for the cationic vacancies is chosen linear, with at both interfaces the

equilibrium concentrations. Figure 3 shows the evolution of the cationic vacancy concentration profile for the 1000 first iterations of the simulation, corresponding to 1.25 s. A curvature appears in the concentration profile near the metal/oxide interface and the vacancies concentration at the interface increases. Indeed, the transfer coefficient is an obstacle to the exchange of cationic vacancies with metallic atoms in the substrate. Then, for longer durations, the cationic vacancies concentration profile keeps on being linear, and the concentration at metal/oxide interface decreases with time toward the equilibrium value (Fig. 4). It has been confirmed that after the transient stage, the cationic vacancy concentration at metal/oxide interface follows the stead-state evolution, given by the following equation [23]:

$$(X_{V_M}^i)_{steady-\atop state} = \frac{D_{V_M} \; X_{V_M}^{eq^s} + \alpha \, e \, X_{V_M}^{eq^i}}{D_{V_M} + \alpha \, e} \tag{8}$$

The shape of the simulated growth kinetics is a complete parabola (t= A + B.e + C.e²) (Fig. 5) as expected from calculation of the steady state case. The kinetics constant evaluated from EKINOX simulations using the analysis given in [24], are k_p =1.30 10^{-11} cm².s⁻¹, and k_l = 1.39 10^{-8} cm.s⁻¹. The small variation between the steady-state and the simulated values comes from the transient stage. This small difference can be even less important if smaller values are chosen for the spatial division step and the time step for the numerical integration.

Table.2 Input data for the simulation of an oxide scale growth controlled by the cationic vacancy diffusion and by the metal transfer at the metal/oxide interface.

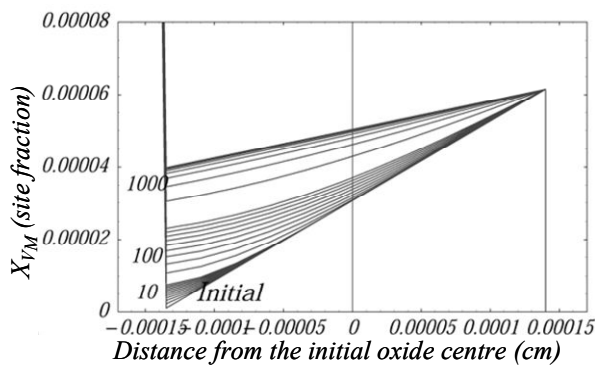| $X_{V_M}^{eq^i}$	$X_{V_M}^{eq^s}$	D_{V_M} (cm².s⁻¹)	k_p (steady-state) (cm².s⁻¹)	α (cm.s⁻¹)	k_l (steady state) (cm.s⁻¹)
10^{-6}	6.15 10^{-5}	1.08 10^{-7}	1.30 10^{-11}	2.15 10^{-4}	1.30 10^{-8}

Fig. 3. Evolution of the cationic vacancies concentration profile during the 1000 first iterations (1.25 s) when the oxide scale growth is controlled by diffusion and interfacial transfer.
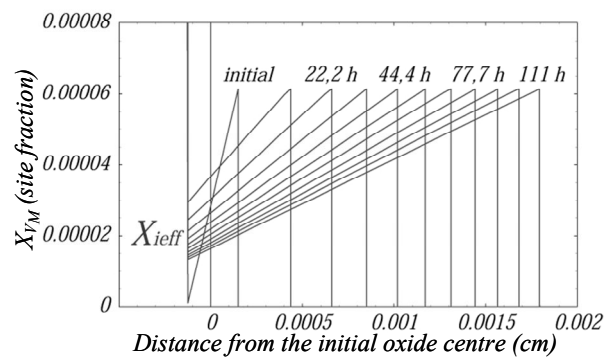

Fig. 4. Evolution of the cationic vacancies concentration profile during the simulation (111 h) when the oxide scale growth is controlled by diffusion and interfacial transfer.

Vacancy concentration profile evolution in the substrate during oxide scale growth. This section illustrates the influence of the hypothesis made for the vacancy treatment on their concentration profile evolution in the substrate. In this case, the oxide scale growth is chosen to be controlled by cationic diffusion (Table 3) and thus the kinetics is parabolic. The data are taken from the literature for the nickel oxide (NiO) growth at 1200°C [22] and metallic vacancy diffusion in pure nickel [16].

Table.3 Input data for the simulation of oxide scale growth controlled by cationic diffusion .

Metallic vacancies		Cationic vacancies		
$X_{V_{Ni}}^{eq}$	$D_{V_{Ni}}$ (cm^2.s^{-1})	$X_{V_{Ni}}^{eq^i}$	$X_{V_{Ni}}^{eq^s}$	$D_{V_{Ni}}$ (cm^2.s^{-1})
3.6 10^{-3}	5 10^{-8}	2 10^{-5}	1.7 10^{-4}	7.57 10^{-7}

Two different hypothesis are made for the vacancy treatment, both considering dislocation density. The first one considers only misfit dislocations at the metal/oxide interface ($\rho_{misfit}=10^{10}$ cm^{-2}), and the second one considers also a non uniform dislocation density in the substrate, decreasing from the surface toward the depth of the substrate, simulating for example the effect of surface cold-working. The dislocation density profile chosen in this case is given on Fig. 6.
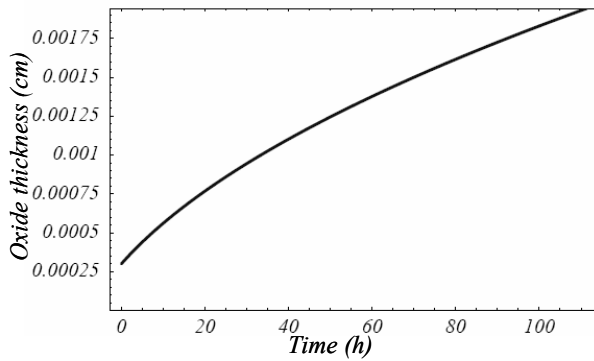

Fig. 5. Calculated oxide scale growth kinetics when controlled by diffusion and interfacial transfer.
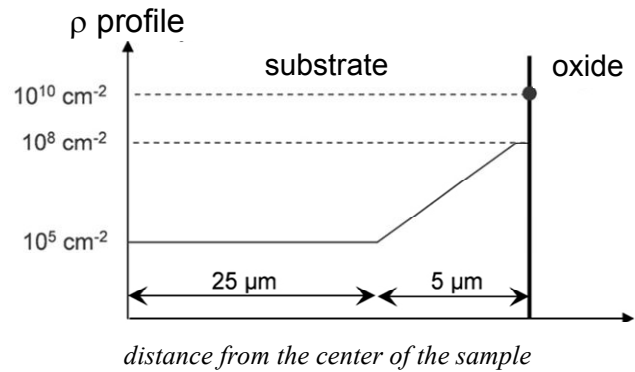

Fig. 6. Schematic representation of the dislocation density profile in the substrate chosen in order to study the evolution of the vacancy concentration.

In the case where only interfacial dislocations are considered, the vacancy concentration profile follows several stages. The whole evolution is given in the reference frame linked to the metal lattice in Fig. 7a. The vacancy concentration first increases in the substrate. Indeed the dislocations are not able to eliminate all the incoming vacancies. Then, when the oxide scale grows, incoming vacancy flux decreases due to the decrease of the concentration gradient in the growing oxide scale. Thus, the misfit dislocations become a sink efficient enough to eliminate all the incoming vacancies. Then, as there is no more vacancy injected in the substrate, the shape of the concentration profile evolves: vacancies that were accumulated in the core of the substrate diffuse backward toward the vacancy sink which is localized at the metal/oxide interface (Fig. 7b). Then the vacancies concentration profile in the substrate becomes flat and the concentration decreases uniformly.
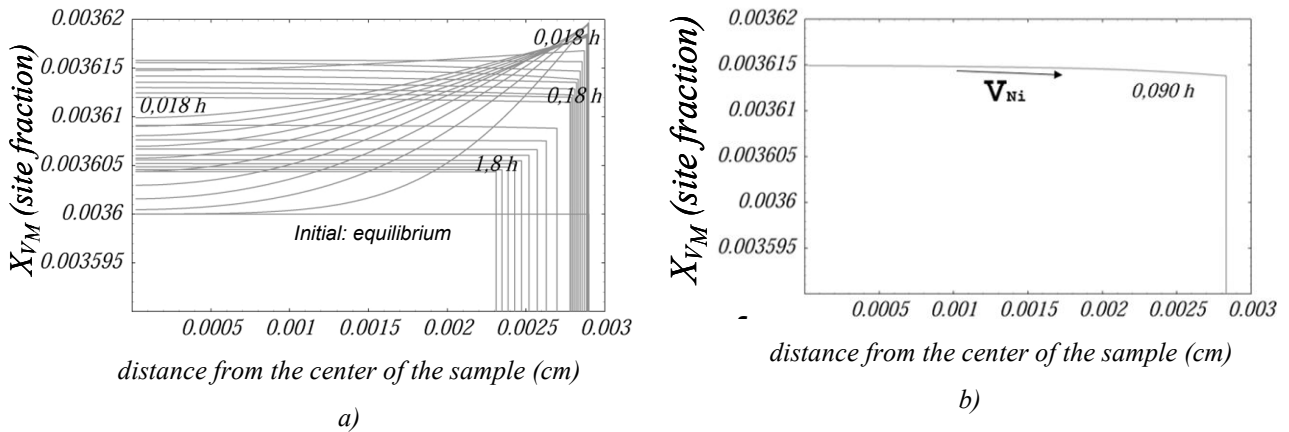
Fig. 7. Evolution of vacancy concentration profile in the substrate in the metallic reference frame when the oxide scale growth is controlled by cationic diffusion and vacancies are eliminated by interfacial dislocations ($\rho_{misfit}=10^{10}$ cm^{-2}) a) entire simulation (1.8 h) – b) intermediate stage of the simulation (0.09 h).

In the second case, vacancy sinks are also distributed in the substrate (Fig. 6), the evolution of the vacancy concentration profile is much simpler as shown in Fig. 8. Indeed, the concentration first increases near the metal/oxide interface because the rate of vacancy injection is initially high. But, those injected vacancies are eliminated in the entire volume of the metal by dislocations and so they do not accumulate in the substrate. Then, at longer durations, the rate of vacancy injection decreases and the concentration profile in the substrate becomes flat and decreases uniformly.
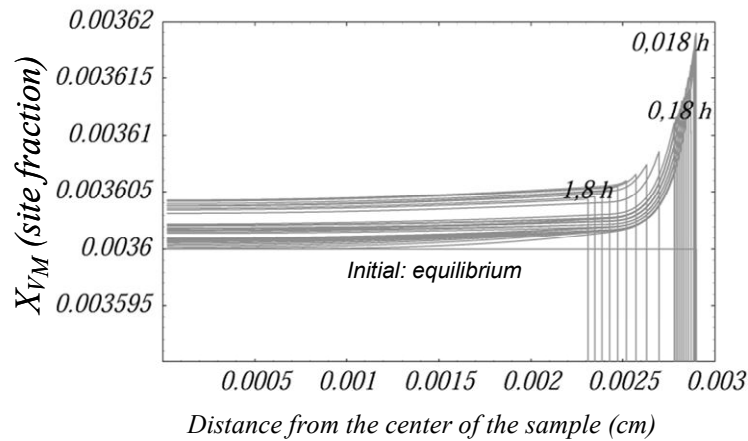

Fig. 8. Evolution of vacancy concentration profile in the substrate (metal lattice as reference frame) when the oxide scale growth is controlled by cationic diffusion and vacancies are eliminated by dislocations (density profile given on Fig. 6).

Finally, these latter simulations results applied in the plain case of a pure metal show that the hypothesis for the treatment of vacancies in the substrate strongly affects the vacancy concentration profile. Vacancy injection could play a major role on the Cr depleted profile in the case of oxidation of Ni-base alloys. However to tackle the case of multi-element alloys, cross-diffusion coefficients in the substrate need to be handled. This can be done following previous work on a model developed to simulate the irradiation assisted segregation at grain boundaries of austenitic steels [25-26].

Future developments: Simulation of the oxidation of an alloy

From now, the EKINOX model will be adapted to simulate the oxidation of an alloy ABC that forms an oxide scale AO_γ. To achieve this goal, the developments are made together with a segregation code already developed for multi-component alloys. This model uses a Self-Consistent Mean Field (SCMF) method to calculate the species and the vacancy transport in the substrate. The atomic diffusion model used in the SCMF model has been validated on different alloy compositions and is now suitable for Ni-base ternary alloys: Ni-Fe-Cr [11, 12]. The diffusion fluxes of the species of the alloy are calculated from a microscopic model of atom-vacancy exchange, which depends on temperature and local composition of the alloy through thermodynamic and kinetic parameters and guarantees a coherent treatment of kinetics and thermodynamics. Thus diffusion coefficients are not extrapolated from high temperature but calculated from the mean exchange frequencies and differences between energy contributions at the saddle point and the initial point, both expressed in terms of nearest neighbor pair interaction energies [11]. The final model reaches a good agreement with the experimental data, as shown in Fig. 9 for binary alloys Ni-Cr, and it predicts that the mean exchange frequencies of Ni, Fe and Cr respectively should stay on a ratio approximately (3,4,9) for any composition, even at lower temperatures [11, 12]. The SCMF model can thus support the development of the EKINOX model for the diffusion in the substrate composed of a ternary alloy ABC (Ni-Fe-Cr).
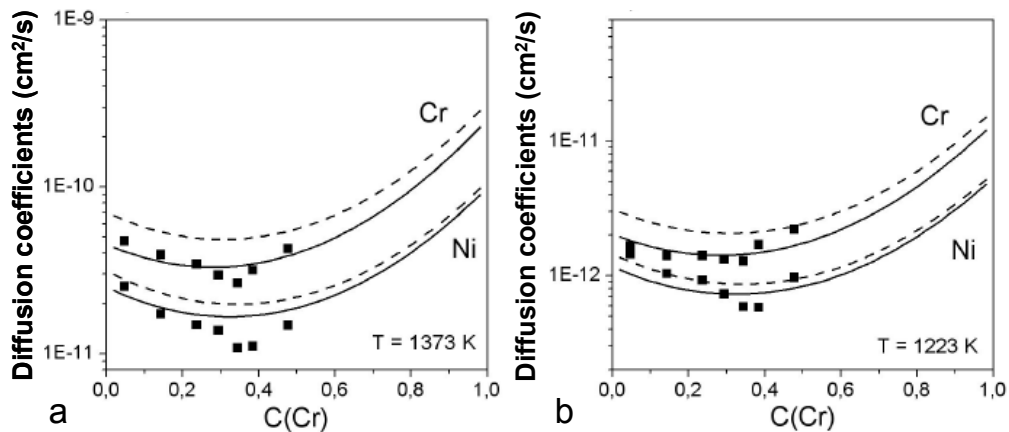

Fig. 9. Tracer diffusion coefficients of Cr and Ni in the Ni-Cr alloy at (a) 1373 K and (b) 1273 K as a function of the composition, obtained experimentally (squares) and by the SCMF model (solid lines). The dotted lines express the non-correlated part of the diffusion coefficients [12].

Conclusion

In order to understand the behavior of nickel based alloys in PWR primary water, the EKINOX numerical model is under development. It simulates an oxide scale growth, taking into account the classical mechanisms of high temperature oxidation, and does not make the classical steady-state hypothesis. The vacancy fluxes are explicitly calculated considering a dislocation distribution acting as vacancy sinks in the substrate. Several EKINOX simulation examples were exposed, in the case of a pure metal, to illustrate different kinds of oxidation kinetics control. It has been shown that whether only interfacial dislocations are taken into account or whether dislocations are also considered in the volume of the substrate, the evolutions of vacancies concentration profiles are strongly different. As vacancy supersaturation and vacancy fluxes should obviously influence the Cr depleted profile in the case of Ni base alloys oxidation, ternary alloys will be handled in future developments, following the SCMF method to calculate the species and vacancies transport in the

substrate. Future simulations will be confronted to experimental studies on oxidation of nickel based alloys (600 and 690) in high temperature water.

References

[1]   P. Combrade, P. M. Scott, M. Foucault, E. Andrieu and P. Marcus, in 12th Int. Conf. on Environmental Degradation of Materials in Nuclear Power Systems-Water Reactors Proceedings, Salt Lake City, Utah, USA 2005.eds.TMS

[2]   L. Marchetti, S. Perrin, O. Raquet, F. Miserque, M. Pijolat, F. Valdivieso and Y. Wouters, in 6th International Symposium on Contribution of Materials Investigations to Improve the Safety and Performance of LWRs Proceedings, Fontevraud , France, 18 - 22 September 2006.

[3]   F. Carrette, M. C. Lafont, G. Chatainier, L. Guinard , B. Pieraggi: Surf. Interf. Anal. Vol.34(1) (2002), p.135

[4]   L. Guinard, O. Kerrec, D. Noel, S. Gardey, F. Coulet: Nucl. Energy Vol.36(11) (1978), p.19

[5]   A. Machet, A. Galtayries, P. Marcus, P. Combrade, P. Jolivet, P. Scott: Surf. Interface Anal., Vol.34(1) (2002), p. 197

[6]   A. Machet, A. Galtayries, A. Zanna, S. Jolivet, P. Foucault, P. Combrade, P. Scott, P. Marcus,
 in EUROCORR 2004 Proceedings; Nice; France; 12-16 Sept. 2004. Eds Maney Publishing (2004).

[7]   J Panter, B Viguier, JM Cloué, M Foucault, P Combrade, E. Andrieu, J. of Nucl. Mat. Vol.48 (1-2) (2006), p.213

[8]   J. Panter, M. Foucault; J.-M. Cloue; P. Combrade; B. Viguier; E. Andrieu, in proceeding of *Corrosion 2002;* Denver, CO; USA; 7-11 Apr. 2002. EdsNACE

[9]   C. Soustelle, M. Foucault, P. Combrade, K. Wolski and T. Magnin, in the Ninth International Symposium on Environmental Degradation of Materials in Nuclear Power Systems - Water Reactors Proceedings, Newport Beach, Ca, USA eds TMS, (1999), p105

[10]   M. Sennour, L. Marchetti, S. Perrin, R. Molins, M. Pijolat and O. Raquet, paper presented at this conference HTCMP 2008

[11]   V. Barbe and M. Nastar, *TMS Letters TMS (The Minerals, Metals and Materials Society)* Vol.2 (2005), p.93

[12]   V. Barbe, PhD Thesis, Centrale Paris (2006). also as *Report CEA-R-6130,* CEA –Saclay, Gif-sur-Yvette (France) (1998).

[13]   M. Seo and N. Sato: Oxid. Met. Vol.19 (1983), p.151.

[14]   M. Seo and N. Sato, in the International Congress on Metallic Corrosion Proceedings, Toronto (Canada), Vol. 2 (1984), p. 362.

[15]   H. W. Pickering and C. Wagner: J. Electrochem. Soc. Vol.114 (1967), p. 698

[16]   S. Perusin, B. Viguier, D. Monceau, L. Ressier, E. Andrieu, Acta Mater.Vol. 52(18) (2004), p.5375

[17]   B. Pieraggi, R. A. Rapp and J. P. Hirth: Oxid. Met. Vol.44 (1995), p.63

[18]   C. Desgranges, N. Bertrand, K. Abbas, D. Monceau and D. Poquillon: Mater. Sci. Forum Vol. 461-464 (2004), p. 481

[19]   C. Desgranges, PhD Thesis, Université Paris XI Orsay (1998) also as *Report CEA-R-5805*, CEA –Saclay, Gif-sur-Yvette (France) (1998).

[20]   D. Monceau and D. Poquillion in *Oxydation des matériaux métalliques,* edited by AM Huntz-Aubriot and B Pieraggi, hermes science publication, Lavoisier, Paris, (2003) p.165

[21]   G. Martin and C. Desgranges: Europhys. Lett. Vol. 44 (1998), p. 150

[22]   S. Mrowec and Z. Grzesik: J.Phy. Chem.Solids Vol.65 (2004), p.1651

[23]   N. Bertrand, PhD Thesis, Institut National Polytechnique de Toulouse (2006).

[24]   D. Monceau and B. Pieraggi: Oxid. Met.Vol.5 0, (1998) p.477

[25]   Y. Grandjean,P. Bellon and G. Martin, Phys.Rev. B Vol. 50 (1994),p. 4228

[26]   M. Nastar: Phil. Mag. Vol.85 (2005), p. 3767